

Design of an LMI-based Polytopic LQR Cruise Controller for an Autonomous Vehicle towards Riding Comfort

Gia Quoc Bao Tran^{1*}, Thanh-Phong Pham², Olivier Sename¹, Péter Gáspár³

¹ GIPSA-lab, CNRS, Grenoble INP, Université Grenoble Alpes, 11 Rue des Mathématiques, 38402 Saint-Martin-d'Hères, France

² Department of Automation, Faculty of Electrical and Electronic Engineering, University of Technology and Education – The University of Danang, 48 Cao Thang street, 550000 Danang, Vietnam

³ Systems and Control Lab, Institute for Computer Science and Control, Hungarian Academy of Sciences, Eötvös Loránd Research Network (ELKH), Kende u. 13-17, H-1111 Budapest, Hungary

* Corresponding author, e-mail: gia-quoc-bao.tran@ieee.org

Received: 01 March 2022, Accepted: 29 June 2022, Published online: 25 August 2022

Abstract

In this paper, we present an LMI-based approach for comfort-oriented cruise control of an autonomous vehicle. First, vehicle longitudinal dynamics and a corresponding parameter-dependent state-space representation are explained and discussed. An LMI-based polytopic LQR controller is then designed for the vehicle speed to track the reference value in the presence of noise and disturbances, where the scheduling parameters are functions of the vehicle mass and the speed itself. An appropriate disturbance force compensation term is also included in the designed controller to provide a smoother response. Then we detail how the reference speed is calculated online, using polynomial functions of the given desired comfort level (quantified by the vertical acceleration absorbed by the human body) and of the road type characterized by road roughness. Finally, time-domain simulations illustrate the method's effectiveness.

Keywords

autonomous vehicle, cruise control, linear parameter-varying (LPV), linear matrix inequality (LMI), gain scheduling, passenger comfort

1 Introduction

Due to the worldwide research interest, nowadays, autonomous vehicles are gaining more and more attention. This is thanks to their capabilities, from collision avoidance (Lunze, 2019) to fuel economy (He et al., 2020), towards safer and greener traffic.

Cruise control refers to adjusting the vehicle speed for various purposes, e.g., collision avoidance, i.e., maintaining a safe distance between vehicles, or fuel consumption reduction, i.e., taking advantage of steep hills. Existing work on cruise control includes several methodologies such as optimal, robust, and LPV control (Gáspár et al., 2017; Kayacan, 2017; Németh and Gáspár, 2011; Öncü et al., 2014; Rajamani and Zhu, 2002). Some work has been linked to the comfort objective (Du et al., 2018; Mohtavipour and Mollajafari, 2021; Schmied et al., 2016).

This article focuses on a Linear Matrix Inequality (LMI) based polytopic LQR cruise control strategy of an autonomous vehicle so as to guarantee riding comfort. Indeed, as detailed by Ahlin and Granlund (2002); Costa et al. (2020) and Loprencipe et al. (2019), there exists a link between

the vehicle speed and the resulting comfort level, characterized by the Root Mean Square (RMS) vertical acceleration absorbed by the passenger, which is caused by road displacements at the four wheels being transmitted through the suspension system (related to vehicle vertical dynamics). This leads to the need of determining and tracking the suitable, comfort-oriented reference speed values for the vehicle, hence the cruise control problem.

This article follows the recent papers of the authors about LPV/ H_2 control with disturbance force compensation (Tran et al., 2021) and a grid-based linear quadratic regulator (LQR) (Tran et al., 2020). Compared with the latter, the LMI conditions for polytopic systems guarantee stability and performance of the closed-loop system for any parameter variation.

The main advantage of this article, compared to other works like Wu et al.'s (2020) article, is that we rely on very basic assumptions for the system, considering benefiting from the knowledge of the vehicle mass using built-in load cells, of the road slope thanks to algorithms such as in the

papers of Li et al. (2017); Vahidi et al. (2005) and Yin et al. (2018), and of the road type thanks to algorithms such as in Tudón-Martínez et al.'s (2015) article. Here, we do not focus on suspension control, but the vertical dynamics still plays an important role in this study in the sense that the pre-computed reference speed functions are obtained from the evaluation of comfort level that was done using the quarter-car model (Costa et al., 2020). The scheduling parameters, in our case, are functions of the vehicle mass and the speed itself (self-scheduling), which allows us to change the representation of the vehicle longitudinal dynamics from a nonlinear one to a linear parameter-varying (LPV) one. An LMI-based optimal controller is then designed by extending existing results of the linear time-invariant (LTI) systems to LPV systems represented in a polytopic form.

This article is organized as follows. Section 2 gives the system modeling where longitudinal dynamics is presented and written into state-space form. An LMI-based polytopic LQR cruise controller is developed in Section 3. In Section 4, we present how riding comfort is quantified and how the reference speed is calculated corresponding to the desired comfort level. In Section 5, we evaluate the control strategy using simulations with different scenarios. Finally, Section 6 gives further analyses and conclusions.

2 System modeling

2.1 Vehicle longitudinal dynamics

Consider an autonomous vehicle of mass m traveling on a road of slope θ at the speed of v . This vehicle is subject to the forces shown in Fig. 1.

The equation of motion is written (Gáspár et al., 2017) for the vehicle as

$$m\dot{v} = F - F_r - F_a - F_g, \quad (1)$$

where F is the longitudinal control force, $F_r = mgC_r \cos\theta$ is the road friction force, $F_a = \frac{1}{2}C_v D_a S v^2$ is the aerodynamic

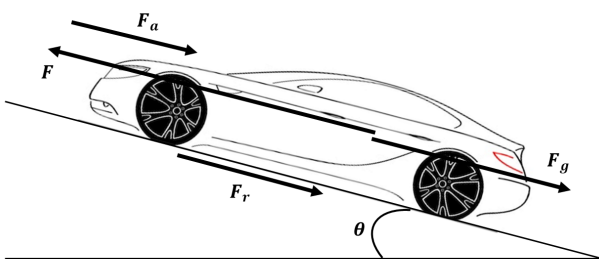


Fig. 1 Longitudinal forces acting on a vehicle

drag, and $F_g = mg \sin\theta \approx mg\theta$ is the gravitational drag. Here g is the gravitational acceleration, C_r is the rolling friction coefficient, C_v is the aerodynamic drag coefficient, D_a is the air density, and S is the vehicle's frontal area. Equation (1) is then rewritten as

$$m\dot{v} = F - mgC_r \cos\theta - \frac{1}{2}C_v D_a S v^2 - mg\theta. \quad (2)$$

Let us assume the following:

- The vehicle mass and speed are measured online thanks to built-in load cells and a speedometer.
- The road slope θ is estimated online as $\hat{\theta}$ using algorithms such as in the papers of Li et al. (2017); Vahidi et al. (2005) and Yin et al. (2018).

Such assumptions allow for disturbance force compensation. The force F has two parts

$$F = F_{ff} + F_{fb}, \quad (3)$$

where $F_{ff} = mg\hat{C}_r \cos\hat{\theta} + mg\hat{\theta}$ is the feed-forward component that compensates for F_r and F_g where \hat{C}_r is the estimated value for C_r , and F_{fb} is the feedback component. As the compensation is inexact, we obtain

$$m\dot{v} = -\frac{1}{2}C_v D_a S v^2 + F_{fb} + m\Delta_{F_{ff}}, \quad (4)$$

where $\Delta_{F_{ff}} = g(\hat{C}_r \cos\hat{\theta} - C_r \cos\theta) + g(\hat{\theta} - \theta)$ is the resulting noise.

2.2 An LPV state-space representation

First, since our objective is to accurately track a reference speed v_{ref} , the system model is extended with an integral term of the tracking error. Therefore, let us introduce a new variable z , where

$$\dot{z} = v_{ref} - v. \quad (5)$$

Following Eq. (4), by choosing $\rho = \begin{bmatrix} 1 & v \\ m & m \end{bmatrix}^T$ as the scheduling parameter vector, we can write the parameter-dependent state-space representation

$$\begin{bmatrix} \dot{v} \\ \dot{z} \end{bmatrix} = \underbrace{\begin{bmatrix} -\frac{1}{2}C_v D_a S \rho_2 & 0 \\ -1 & 0 \end{bmatrix}}_{A(\rho)} \begin{bmatrix} v \\ z \end{bmatrix} + \underbrace{\begin{bmatrix} \rho_1 \\ 0 \end{bmatrix}}_{B(\rho)} F_{fb} + \underbrace{\begin{bmatrix} 0 \\ 1 \end{bmatrix}}_{B_1} v_{ref} + \underbrace{\begin{bmatrix} 1 \\ 0 \end{bmatrix}}_{B_2} \Delta_{F_{ff}},$$

$$y = \underbrace{\begin{bmatrix} 1 & 0 \end{bmatrix}}_C \begin{bmatrix} v \\ z \end{bmatrix}, \quad (6)$$

(6)

which is then rewritten as

$$\begin{aligned} \dot{\mathbf{x}} &= \mathbf{A}(\boldsymbol{\rho})\mathbf{x} + \mathbf{B}(\boldsymbol{\rho})u + \mathbf{B}_1r + \mathbf{B}_2w, \\ y &= \mathbf{C}\mathbf{x}, \end{aligned} \quad (7)$$

where $\mathbf{x} = [v \ z]^T$ is the state vector, $u = F_{fb}$ is the control input, $r = v_{ref}$ is the reference, $w = \Delta_{F_{ff}}$ is the noise, and $y = v$ is the measured output. In this representation, $\boldsymbol{\rho}$ is known/estimated and is bounded, i.e., $\boldsymbol{\rho} \in [\underline{\boldsymbol{\rho}}, \bar{\boldsymbol{\rho}}]$.

It is worth noting that the system in Eq. (6) is referred to as a quasi-LPV system since the parameter vector depends on the state variable.

Values of the parameters are presented in Table 1.

The mass is assumed constant while the vehicle is traveling, but it can be different for each run (depending on the number of passengers and amount of luggage). Besides, the speed is bounded in $[0, 35]$ m/s.

Note that we consider the maximum value (in magnitude) for the longitudinal control force as 4000 N.

3 LMI-based polytopic LQR cruise control

In this part, the cruise controller is designed as a state-feedback LPV optimal controller. Such a design method is performed in the LMI framework, allowing us to extend well-known results for LTI systems to LPV ones. Those main results are detailed in Proposition 1.

Proposition 1 (de Souza et al., 2003; Xie, 2005): *Consider the following system, control input, and cost function*

$$\begin{aligned} \dot{\mathbf{x}} &= \mathbf{A}(\boldsymbol{\rho})\mathbf{x} + \mathbf{B}\mathbf{u} + \mathbf{B}_w\mathbf{w}, \\ \mathbf{z} &= \mathbf{C}_z\mathbf{x} + \mathbf{D}_z\mathbf{u}, \\ \mathbf{u} &= -\mathbf{K}(\boldsymbol{\rho})\mathbf{x}, \\ J &= \min_u \int_0^{+\infty} \mathbf{z}^T \mathbf{z} \, dt, \end{aligned} \quad (8)$$

where \mathbf{x} is the state, \mathbf{w} is noise, \mathbf{z} is the controlled output, $\boldsymbol{\rho}$ is a vector of N scheduling scalar parameters. Note that \mathbf{B} needs to be parameter-independent. The state-feedback controller gain $\mathbf{K}(\boldsymbol{\rho})$ that stabilizes the system in Eq. (8) is found, minimizing the cost J , in a three-step procedure.

Table 1 Parameter values

Symbol	Value	SI unit
m	[1400, 1680]	kg
C_r	0.01	-
C_v	0.32	-
D_a	1.3	kg/m ³
S	2.4	m ²
g	9.8	m/s ²

Let $\boldsymbol{\omega}_i$ be a vertex of $\boldsymbol{\rho}$, $i = 1, 2, \dots, 2^N$. First, we solve for matrices \mathbf{Y}_i , \mathbf{W}_i , and a positive-definite matrix \mathbf{P} , minimizing $\gamma > 0$ s.t

$$\begin{aligned} \mathbf{A}(\boldsymbol{\omega}_i)\mathbf{P} + \mathbf{P}\mathbf{A}^T(\boldsymbol{\omega}_i) + \mathbf{B}_i(\boldsymbol{\omega}_i)\mathbf{Y}_i + \mathbf{Y}_i^T\mathbf{B}_i^T(\boldsymbol{\omega}_i) + \mathbf{B}_w\mathbf{B}_w^T &< 0, \\ \begin{bmatrix} \mathbf{P} & \mathbf{P}\mathbf{C}_z^T + \mathbf{Y}_i^T\mathbf{D}_z^T \\ \mathbf{C}_z\mathbf{P} + \mathbf{D}_z\mathbf{Y}_i & \mathbf{W}_i \end{bmatrix} &> 0, \\ \text{tr}(\mathbf{W}_i) &< \gamma^2, \quad \forall i. \end{aligned} \quad (9)$$

Then, $\mathbf{K}_i = \mathbf{Y}_i\mathbf{P}^{-1}$ is the controller corresponding to the LTI system at vertex $\boldsymbol{\omega}_i$. Finally, since the system in Eq. (8) is parameter-independent in the control input, $\mathbf{K}(\boldsymbol{\rho})$ is found using the polytopic method as

$$\mathbf{K}(\boldsymbol{\rho}) = \sum_i^{2^N} \alpha_i(\boldsymbol{\rho}) \mathbf{K}_i, \quad (10)$$

where $\alpha_i(\boldsymbol{\rho}) > 0, \forall i$ and $\sum_i^{2^N} \alpha_i(\boldsymbol{\rho}) = 1$ are the interpolation functions for gain scheduling.

Proof: The proof is available in the works of de Souza et al. (2003) and Xie (2005). This is applied here to polytopic systems, in the framework of quadratic stability, so considering a single Lyapunov function.

For controller design, the system in Eq. (7) is first written in a polytopic form as in Apkarian et al.'s (1995) article, so that the state matrix now writes $\mathbf{A}(\boldsymbol{\rho}) = \sum_i^{2^N} \alpha_i(\boldsymbol{\rho}) \mathbf{A}_i$.

Note that, since the input matrix must be parameter-independent to apply the polytopic method, while the system in Eq. (7) has a parameter-dependent control input matrix, we need to add the following filter to the input matrix as explained by Apkarian et al. (1995):

$$\begin{aligned} \dot{x}_f &= A_f x_f + B_f u_f, \\ u &= C_f x_f, \end{aligned} \quad (11)$$

where $A_f = -1/\tau_f$, $B_f = 1/\tau_f$, $C_f = 1$ where τ_f is a small constant. The system in Eq. (7) is then extended into

$$\begin{aligned} \begin{bmatrix} \dot{\mathbf{x}} \\ \dot{x}_f \end{bmatrix} &= \begin{bmatrix} \mathbf{A}(\boldsymbol{\rho}) & \mathbf{B}(\boldsymbol{\rho})C_f \\ 0 & A_f \end{bmatrix} \begin{bmatrix} \mathbf{x} \\ x_f \end{bmatrix} + \begin{bmatrix} 0 \\ B_f \end{bmatrix} u_f + \begin{bmatrix} \mathbf{B}_1 \\ 0 \end{bmatrix} r \\ &+ \begin{bmatrix} \mathbf{B}_2 \\ 0 \end{bmatrix} w, \\ y &= [C \ 0] \begin{bmatrix} \mathbf{x} \\ x_f \end{bmatrix}, \end{aligned} \quad (12)$$

where u_f is the new, parameter-independent control input.

Remark 1: It is worth noticing that the above results ensure stability and performance of the closed-loop LPV system for any parameter variation.

Remark 2: If C_z and D_z are full-rank matrices and satisfy $C_z^T D_z = 0$, then the cost function J is an LQR one where $Q = C_z^T C_z > 0$ and $R = D_z^T D_z > 0$.

Remark 3: The matrix B_w is appropriately chosen to normalize the effect of the noise w on the system dynamics, avoiding being overly conservative.

Proposition 1 is then applied to the system in Eq. (12) to find the cruise controller. We choose $\tau_f = 0.001$ s for the filter in Eq. (11), and the matrices C_z and D_z as

$$C_z = \begin{bmatrix} 1 & 0 & 0 \\ 0 & 5 & 0 \\ 0 & 0 & 10^{-6} \\ 0 & 0 & 0 \end{bmatrix}, \quad D_z = \begin{bmatrix} 0 \\ 0 \\ 0 \\ 0.01 \end{bmatrix}, \quad (13)$$

to lay greater emphasis on the integral of the tracking error.

4 Comfort-oriented reference speed calculation

4.1 Evaluation of comfort level

The road is classified into different types, defined by the ISO 8608:2016 standard (ISO, 2016). It is known that the road displacements at the four wheels depend not only on the road type but on the vehicle speed as well. In Fig. 2, we show various road displacement profiles corresponding to the constant speed of 12 m/s, with different road types A–D.

The displacements/vibrations are transmitted to passengers through vehicle vertical dynamics, causing driving discomfort due to vertical acceleration. The riding comfort of onboard passengers is thus quantified by the RMS of the vertical acceleration filtered by Zuo and Nayfeh (2003):

$$W_{ISO} = \frac{81.89s^3 + 796.6s^2 + 1937s + 0.1446}{s^4 + 80s^3 + 2264s^2 + 7172s + 21196}, \quad (14)$$

which serves to model human perception of acceleration. The comfort levels are evaluated according to the ISO 2631-1:1997 standard (ISO, 1997) as listed in Table 2.

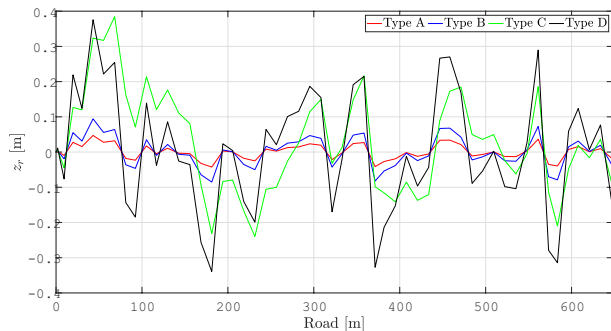


Fig. 2 Road displacement for types A–D for a speed of 12 m/s

4.2 Comfort-guaranteeing reference speed

Our research group has proposed a method (in Costa et al.'s (2020) work) to compute the reference speed value given the estimated road type and desired comfort level using polynomials. We experimented with different road types and speed values using a quarter-car model, then obtained and related the calculated comfort criteria with the vehicle speed (see Fig. 3).

Then, a fitting method was used to find the polynomials (see Table 3) that gave us the suitable reference speed values from the desired comfort level (characterized by the RMS acceleration specified by passengers) for each road type A–D.

These polynomial functions are precomputed and programmed into the vehicle for online calculation of the comfort-oriented reference speed. Indeed, in practice, the road type can be estimated thanks to estimation algorithms such as in Tudón-Martínez et al.'s (2015) article.

Table 2 Evaluation of riding comfort from RMS acceleration

RMS value	Evaluation of comfort
Less than 0.315 m/s ²	Not uncomfortable
0.315–0.63 m/s ²	A little uncomfortable
0.5–1 m/s ²	Fairly uncomfortable
0.8–1.6 m/s ²	Uncomfortable
1.25–2.5 m/s ²	Very uncomfortable
Greater than 2 m/s ²	Extremely uncomfortable

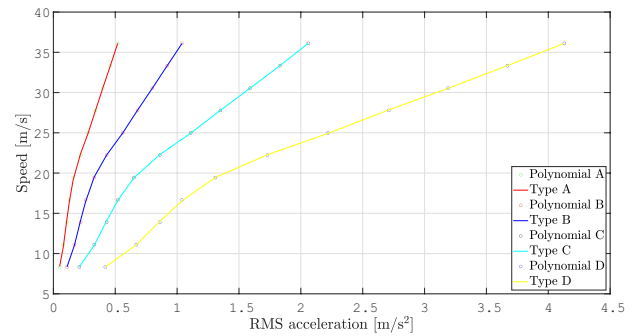


Fig. 3 Comfort-guaranteeing reference speed polynomials

Table 3 Comfort-oriented reference speed polynomials

Road type	Comfort-oriented reference speed function $v_{ref}(q)$ where q is RMS acceleration
A	$-281058.82q^7 + 616932.65q^6 - 553287.74q^5 + 259269.77q^4 - 67006.34q^3 + 9126.1q^2 - 490.82q + 17.03$
B	$-2918.46q^7 + 12566.60q^6 - 22133.93q^5 + 20420.08q^4 - 10438.88q^3 + 2839.03q^2 - 319.40q + 20.36$
C	$-20.58q^7 + 176.82q^6 - 620.95q^5 + 1140.85q^4 - 1158.9q^3 + 623.06q^2 - 134.38q + 17.84$
D	$-0.19q^7 + 3.22q^6 - 22.33q^5 + 81.06q^4 - 162.92q^3 + 174.09q^2 - 76.47q + 19.57$

5 Simulation results

In this part, the proposed cruise control method is validated through time-domain simulations using different scenarios.

5.1 Simulation scenario 1

Consider a vehicle mass of 1680 kg (maximum). In this 300-second long scenario, as shown in Fig. 4 and Fig. 5:

- The comfort level (characterized by the desired RMS acceleration) decreases from 0.3 m/s² to 0.2 m/s² at 60 s (about 600 m), then increases to 0.4 m/s² at 180 s (about 2300 m), and then decreases to 0.3 m/s² at 240 s (about 4200 m).
- The road type (characterized by the estimated road roughness) changes from B to A at 120 s (about 1100 m) and back to B at 240 s (about 4200 m).

The resulting reference and vehicle speed are shown in Fig. 6, while the longitudinal control force is shown in Fig. 7.

We see that under disturbances, the tracking is achieved after around 200 m, with a limited control force.

5.2 Simulation scenario 2

This second scenario is dedicated to robustness assessment of the controlled system considering inadequate knowledge of some system parameters, which are called uncertain parameters. Consider the vehicle mass of 1470 kg and

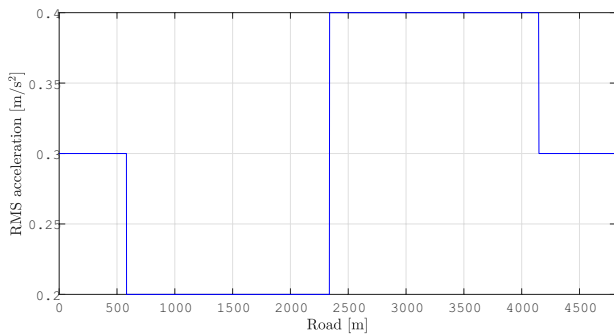


Fig. 4 Simulation scenario 1: Desired RMS acceleration

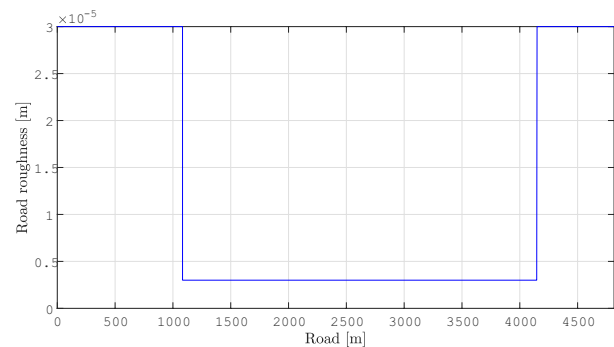


Fig. 5 Simulation scenario 1: Road roughness

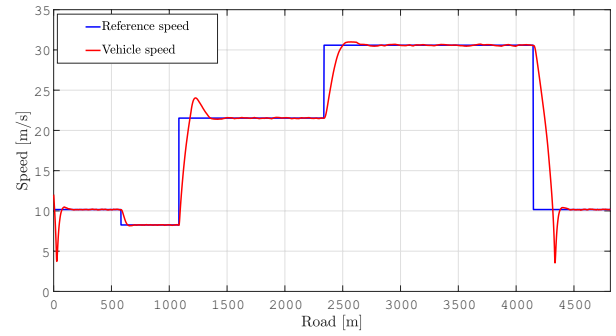


Fig. 6 Simulation scenario 1: Resulting reference and vehicle speed

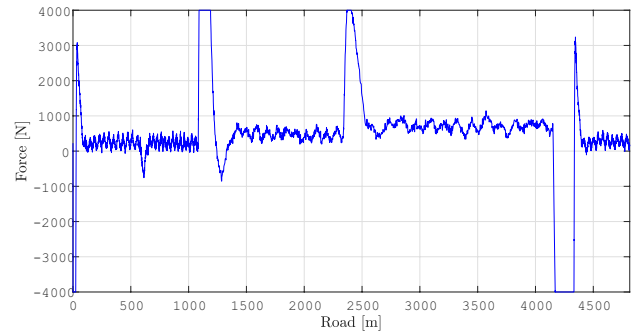


Fig. 7 Simulation scenario 1: Longitudinal control force

the rolling friction coefficient $C_r = 0.01 \pm 10\%$ as an uncertain parameter.

In this 120-second long scenario, as shown in Fig. 8 and Fig. 9:

- The comfort level (characterized by the desired RMS acceleration) increases from 0.2 m/s² to 0.4 m/s² at 24 s (about 450 m), then decreases to 0.3 m/s² at 72 s (about 1600 m), and then decreases to 0.2 m/s² at 96 s (about 1800 m).
- The road type (characterized by the estimated road roughness) changes from A to B at 48 s (about 1200 m) and back to A at 96 s (about 1800 m).

The resulting reference and vehicle speed are shown in Fig. 10, while the longitudinal control force is shown in Fig. 11.

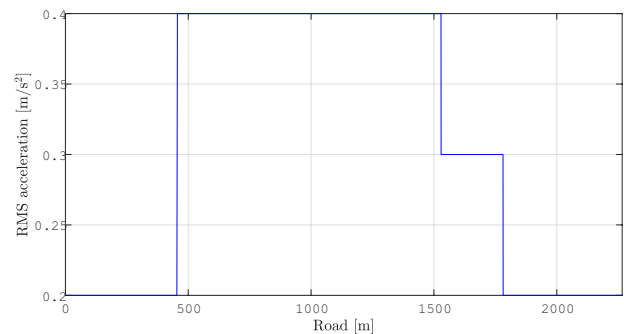


Fig. 8 Simulation scenario 2: Desired RMS acceleration

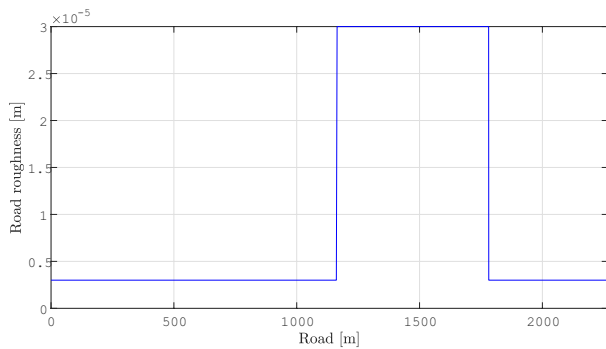


Fig. 9 Simulation scenario 2: Road roughness

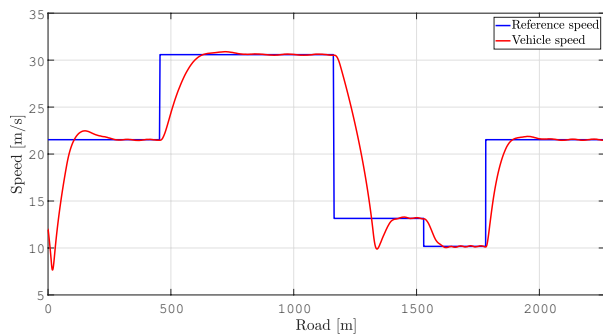


Fig. 10 Simulation scenario 2: Resulting reference and vehicle speed

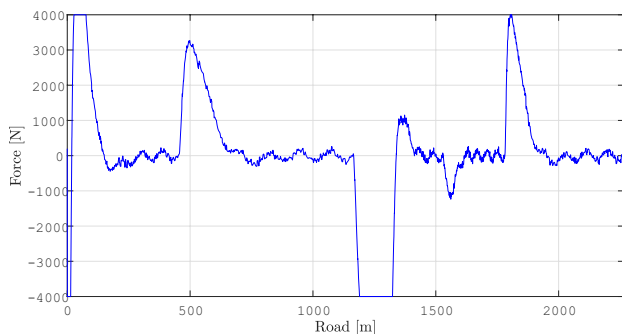


Fig. 11 Simulation scenario 2: Longitudinal control force

References

Ahlin, K., Granlund, J. (2002) "Relating Road Roughness and Vehicle Speeds to Human Whole Body Vibration and Exposure Limits", *International Journal of Pavement Engineering*, 3(4), pp. 207–216. <https://doi.org/10.1080/10298430210001701>

Apkarian, P., Gahinet, P., Becker, G. (1995) "Self-scheduled H_∞ Control of Linear Parameter-varying Systems: A Design Example", *Automatica*, 31(9), pp. 1251–1261. [https://doi.org/10.1016/0005-1098\(95\)00038-X](https://doi.org/10.1016/0005-1098(95)00038-X)

Costa, E., Pham, T.-P., Sename, O., Tran, G. Q. B., Do, T. T., Gaspar, P. (2020) "Definition of a Reference Speed of an Autonomous Vehicle with a Comfort Objective", presented at VSDIA 2020 – 20th International Conference on Vehicle System Dynamics, Identification and Anomalies, Budapest, Hungary, Nov., 10–12.

de Souza, C. E., Trofino, A., de Oliveira, J. (2003) "Parametric Lyapunov Function Approach to H_2 Analysis and Control of Linear Parameter-dependent Systems", *IEE Proceedings - Control Theory and Applications*, 150(5), pp. 501–508. <https://doi.org/10.1049/ip-cta:20030709>

We see that when the rolling friction coefficient is considered uncertain, the controlled system still achieves a satisfactory tracking performance with a limited control force.

The two simulation scenarios show that the cruise control strategy works and is robust enough w.r.t the considered level of uncertainty.

6 Conclusion

This article proposes a state-feedback cruise controller using an LMI-based LPV LQR method under the polytopic approach, which is effective and robust w.r.t disturbances and uncertainty. Combined with the comfort-oriented reference speed calculation strategy, it allows us to guarantee passenger riding comfort.

Further research on comfort-oriented vehicle control can be conducted using machine learning algorithms in order to take into account several types of data coming from the vehicles and infrastructure.

Acknowledgement

This research work has been supported by the PHC BALATON project under project number 41854PM.

Du, Y., Liu, C., Li, Y. (2018) "Velocity Control Strategies to Improve Automated Vehicle Driving Comfort", *IEEE Intelligent Transportation Systems Magazine*, 10(1), pp. 8–18. <https://doi.org/10.1109/MITS.2017.2776148>

Gáspár, P., Szabó, Z., Bokor, J., Németh, B. (2017) "Robust Control Design for Active Driver Assistance Systems: A Linear-Parameter-Varying Approach", [e-book] Springer. ISBN 978-3-319-46126-7 <https://doi.org/10.1007/978-3-319-46126-7>

He, C. R., Ge, J. L., Orosz, G. (2020) "Fuel Efficient Connected Cruise Control for Heavy-Duty Trucks in Real Traffic", *IEEE Transactions on Control Systems Technology*, 28(6), pp. 2474–2481. <https://doi.org/10.1109/TCST.2019.2925583>

International Organization for Standardization (1997) "ISO 2631-1:1997 Mechanical Vibration and Shock - Evaluation of Human Exposure to Whole Body Vibration - Part 1: General Requirements", ISO, Geneva, Switzerland. [online] Available at: <https://www.iso.org/standard/7612.html> [Accessed: 25 March 2021]

- International Organization for Standardization (2016) "ISO 8608:2016 Mechanical Vibration - Road Surface Profiles - Reporting of Measured Data", ISO, Geneva, Switzerland. [online] Available at: <https://www.iso.org/standard/71202.html> [Accessed: 25 March 2021]
- Kayacan, E. (2017) "Multiobjective H_{∞} Control for String Stability of Cooperative Adaptive Cruise Control Systems", *IEEE Transactions on Intelligent Vehicles*, 2(1), pp. 52–61. <https://doi.org/10.1109/TIV.2017.2708607>
- Li, B., Zhang, J., Du, H., Li, W. (2017) "Two-layer Structure Based Adaptive Estimation for Vehicle Mass and Road Slope under Longitudinal Motion", *Measurement*, 95, pp. 439–455. <https://doi.org/10.1016/j.measurement.2016.10.045>
- Loprencipe, G., Zoccali, P., Cantisani, G. (2019) "Effects of Vehicular Speed on the Assessment of Pavement Road Roughness", *Applied Sciences*, 9(9), 1783. <https://doi.org/10.3390/app9091783>
- Lunze, J. (2019) "Adaptive Cruise Control With Guaranteed Collision Avoidance", *IEEE Transactions on Intelligent Transportation Systems*, 20(5), pp. 1897–1907. <https://doi.org/10.1109/TITS.2018.2842115>
- Mohtavipour, S. M., Mollajafari, M. (2021) "An Analytically Derived Reference Signal to Guarantee Safety and Comfort in Adaptive Cruise Control Systems", *Journal of Intelligent Transportation Systems*, 25(1), pp. 1–20. <https://doi.org/10.1080/15472450.2019.1619559>
- Németh, B., Gáspár, P. (2011) "LPV-based Control Design of Vehicle Platoon Considering Road Inclinations", *IFAC Proceedings Volumes*, 44(1), pp. 3837–3842. <https://doi.org/10.3182/20110828-6-IT-1002.00933>
- Öncü, S., Ploeg, J., van de Wouw, N., Nijmeijer, H. (2014) "Cooperative Adaptive Cruise Control: Network-aware Analysis of String Stability", *IEEE Transactions on Intelligent Transportation Systems*, 15(4), pp. 1527–1537. <https://doi.org/10.1109/TITS.2014.2302816>
- Rajamani, R., Zhu, C. (2002) "Semi-autonomous Adaptive Cruise Control Systems", *IEEE Transactions on Vehicular Technology*, 51(5), pp. 1186–1192. <https://doi.org/10.1109/TVT.2002.800617>
- Schmied, R., Waschl, H., del Re, L. (2016) "Comfort Oriented Robust Adaptive Cruise Control in Multi-Lane Traffic Conditions", *IFAC-PapersOnLine*, 49(11), pp. 196–201. <https://doi.org/10.1016/j.ifacol.2016.08.030>
- Tran, G. Q. B., Pham, T.-P., Sename, O., Costa, E., Gaspar, P. (2021) "Integrated Comfort-Adaptive Cruise and Semi-Active Suspension Control for an Autonomous Vehicle: An LPV Approach", *In: Electronics*, 10(7), 813. <https://doi.org/10.3390/electronics10070813>
- Tran, G. Q. B., Sename, O., Gáspár, P., Németh, B., Costa, E. (2020) "Adaptive Speed Control of an Autonomous Vehicle with a Comfort Objective", presented at VSDIA 2020 – 20th International Conference on Vehicle System Dynamics, Identification and Anomalies, Budapest, Hungary, Nov., 10–12.
- Tudón-Martínez, J. C., Fergani, S., Sename, O., Martínez, J. J., Morales-Menendez, R., Dugard, L. (2015) "Adaptive Road Profile Estimation in Semiactive Car Suspensions", *IEEE Transactions on Control Systems Technology*, 23(6), pp. 2293–2305. <https://doi.org/10.1109/TCST.2015.2413937>
- Vahidi, A., Stefanopoulou, A., Peng, H. (2005) "Recursive Least Squares with Forgetting for Online Estimation of Vehicle Mass and Road Grade: Theory and Experiments", *Vehicle System Dynamics*, 43(1), pp. 31–55. <https://doi.org/10.1080/00423110412331290446>
- Wu, J., Zhou, H., Liu, Z., Gu, M. (2020) "Ride Comfort Optimization via Speed Planning and Preview Semi-active Suspension Control for Autonomous Vehicles on Uneven Roads", *IEEE Transactions on Vehicular Technology*, 69(8), pp. 8343–8355. <https://doi.org/10.1109/TVT.2020.2996681>
- Xie, W. (2005) "H2 Gain Scheduled State Feedback for LPV System with New LMI Formulation", *IEE Proceedings – Control Theory and Applications*, 152(6), pp. 693–697. <https://doi.org/10.1049/ip-cta:20050052>
- Yin, Z., Dai, Q., Guo, H., Chen, H., Chao, L. (2018) "Estimation Road Slope and Longitudinal Velocity for Four-wheel Drive Vehicle", *IFAC-PapersOnLine*, 51(31), pp. 572–577. <https://doi.org/10.1016/j.ifacol.2018.10.139>
- Zuo, L., Nayfeh, S. (2003) "Low Order Continuous-time Filters for Approximation of the ISO 2631-1 Human Vibration Sensitivity Weightings", *Journal of Sound and Vibration*, 265(2), pp. 459–465. [https://doi.org/10.1016/S0022-460X\(02\)01567-5](https://doi.org/10.1016/S0022-460X(02)01567-5)